

**Investigation into Low Energy Beta Imaging Using CCD
Imaging Sensor**

117

Suhairul Hashim

**A dissertation is submitted to the Department of Physics,
University of Surrey, in partial fulfilment of the Degree of
Master of Science in Medical Physics**

**Department of Physics
School of Electronics and Physical Sciences
University of Surrey
September 2004
©Suhairul Hashim**

Abstract

Autoradiography is an extensively used technique to create a record of the radioactivity dispersion throughout the biological samples. Conventionally, this technique was performed using film. Spatial resolution and sensitivity are the main parameters of interest in developing new digital autoradiography systems. In conventional autoradiography, the images that have been documented display an excellent spatial resolution but at the same time show lack of sensitivity, very limited dynamic range and non-linear response. To overcome the disadvantages of this method, digital autoradiography systems have been developed to address the major drawbacks of the former technique.

This thesis is focussed in a method of imaging the beta emissions from radiolabelled tissue specimens that has been developed by using a CCD imaging sensor. Most of the work involving autoradiography techniques is conducted using beta emitters such as ^3H and ^{14}C because of their occurrence in abundance in organic materials. Thus, the work in this project is to develop a method for imaging these very low energy emissions for ^{14}C where the end point energy around 156 keV. Preliminary calculations suggest that by using scintillator paper, then such an approach would open up the way for dual tracer imaging. It also involves learning aspects of applying CCD imaging system to compare the images acquired from ^{14}C and ^{241}Am sources either using scintillator paper or without it. Finally, preliminary results demonstrate that this approach may will be feasible based on the perceived images from the experiment.

Acknowledgements

It is a great pleasure to address those people who helped me throughout this project to enhance my knowledge and practical skills especially in research area. I am most grateful to have Dr. Kevin Wells as my supervisor because of his concern, experiences, moral supports, guidance, help, explanation and advices. To Mr. Denis Libaert and Mrs. Liz Griffiths for helping me in experimental works, Mr. Daniel, Mr. Hezerul and Mr. Iqbal for guiding me in Mathlab software.

Many thanks specifically to my sponsorship, Universiti Teknologi Malaysia and generally to Malaysia Government for giving me a great chance to pursue my study in University of Surrey.

I wish to express my special thanks to my beloved parents Hjh. Sapiyah Hasan and Hj. Hashim Ahmad, all my siblings Abg. Mie, Kak Ana, Abg. Yie, Izal, Kak Zai, Kak Nora and Abg. Nahar and for my special, Sitti Asmah Hassan, for all the prayers and supports you have made for me. Finally, to all Malaysian in University of Surrey and my respectful classmates, always remember our greatest moment either happiness or tears for almost one year.

This project would have been impossible without your guidance, advice and support. May God bless our life throughout the years and here after.

.....To my family
For your encouragement and support

Table of contents

Chapter 1 - Introduction

1.1	Overview.....	1
1.2	Components of Autoradiography	
1.2.1	Specimen / sample.....	1
1.2.2	Radionuclides.....	2
1.2.3	Film.....	3
1.3	Techniques of Conventional Autoradiography.....	4
1.4	Advantages and disadvantages of Conventional Autoradiography.....	7
	References.....	9

Chapter 2 – Digital autoradiography

2.1	Introduction.....	10
2.2	Phosphor imaging plates.....	11
2.3	Silicon hybrid pixels detectors.....	12
2.4	Multiwire proportional chamber.....	13
2.5	Microchannel plates.....	14
2.6	Charge-coupled devices.....	15
2.7	Scintillator combinations.....	16
2.8	Summary.....	19
	References.....	20

Chapter 3 – Charge-coupled devices

3.1	Introduction.....	22
3.2	Components and principles of CCD.....	22
3.3	CCD architectures.....	23
	References.....	28

Chapter 4 – Methodology and System Description

4.1	Introduction.....	29
4.2	System description.....	29
4.3	The CCD sensor.....	30
4.4	Interval generator.....	31
4.5	PCI MIO connector.....	32
4.6	PC and data acquisition card.....	32
4.7	Software.....	32
4.8	Installation of a CCD device.....	33
4.9	Preparing ^{14}C microscales.....	36
4.10	Estimation of the signal generated in CCD sensor.....	37
4.11	Post-acquisition processing.....	39
	References.....	40

Chapter 5 – Results and Discussion

5.1	Introduction.....	41
5.2	The dark current effects.....	41
5.3	Image acquisition.....	43
	References.....	49

Chapter 6 – Conclusion and Future work

6.1	Conclusion.....	50
6.2	Future work.....	51

Appendices

Appendix A: CCD05-20 Data Sheet.....	52
Appendix B: Switch positions on the Digital Board.....	58
Appendix C: 14C Microscales Source Data Sheet.....	60
Appendix D: Mathlab Code for Image Acquisition Processing.....	65
Appendix E: P-47 Phosphor / Scintillator Data Sheet.....	67

List of Figures

- **Figure 1.2.1:1:** Autoradiography process involves specimen, tracer and detector to form the image [BAK, 1989].....2

- **Figure 1.2.3:1:** Cross-section of double coated photographic emulsion illustrating the base, emulsion and supercoat. The emulsion is attached to the base by a thin layer of adhesive [GAM, 2004].....4

- **Figure 1.2.3:2:** Silver halide crystal lattice structure showing the relative locations of Br⁻, Ag⁺ and I⁻ ions [GAM, 2004].....4

- **Figure 1.3:1:** The effect of slice thickness on resolution. Emission sources that are distant from the photographic film (as in thick slices) may expose a broader area of the emulsion than sources that are close [GAM, 2004].....6

- **Figure 1.3:2:** The effect of energy and tissue thickness on resolution. The top row of sections uses the low-energy emitter ¹⁴C as a tracer; the bottom row uses the higher-energy emitter ¹⁸F. Thicknesses of the sections in both rows are 20, 40, 120, and 180 μm from left to right. Resolution is degraded for the higher-energy emitter and diminishes as tissue thickness increases [GAM, 2004].....6

- **Figure 1.3:3:** Distribution of tracks versus energy for microautoradiography. $d / (d)^{1/2}$ is the distance between a developed grain and its radioactive source divided by the median distance of all developed grains. The graph implies that it is more difficult to determine the origin of high-energy electron emitters than low-energy electron emitters due to longer tracks and wider track scattering [GAM, 2004].....7

- **Figure 2.2:1:** Microscopic cross section images captured by phosphor layer after exposing the plate. The exposed IP is scanned with a focused laser beam. The photostimulated luminescence released upon the laser is collected into the PMT through the light collection guide and is converted to electric signals [GAM, 2004].....11

- **Figure 2.3:1:** The Medipix2 chip main components include semiconductor sensor chip, flip-chip bump bonding connections, CMOS pixel read-out chip and single pixel read-out cell [MED, 2004].....13
- **Figure 2.4:1:** Multiwire proportional chamber consist of anode wire and cathode planes.....14
- **Figure 2.5:1:** Schematic of the microchannel detector showing the sample (electrophoresis gel) being driven to imaging position. Efficient imaging requires the sample to be presented to the detector inside the vacuum chamber using automatic sample loading and vacuum load-lock mechanism [JEL, 1999].....15
- **Figure 2.6:1:** Block diagram of the prototype CCD system [MAC, 1996].....16
- **Figure 2.7:1:** Components of Beta camera comprises scintillator, optical coupling agent, fibre optic face-plate, photocathode surface, microchannel plates and resistive anode [FAD, 2003].....17
- **Figure 2.7:2:** General operating principles of β -imager and of μ -imager. Beta Imager based on gaseous scintillation has very wide field of view 20 cm x 25 cm enable to image small sections of sample. Micro-Imager offers high resolution but has limited field of view 2.4 cm x 3.2 cm [BAR, 2004].....18
- **Figure 3.2:1:** A charge-coupled devices [FAD, 2003].....23
- **Figure 3.2:2:** Potential well and potential barriers [KOD, 2004].....23
- **Figure 3.3:1:** Full-Frame Architecture consist of a parallel, serial CCD shift register and a signal sensing output amplifier [KOD, 2004].....24

• Figure 3.3:2: Read out of CCD area array. The CCD transfers packets of electrons along its vertical and horizontal registers as an analogue signal. The output electrons signal is converted to a change in output voltage [KEV, 2004].....	24
• Figure 3.3:3: Frame-Transfer Architecture [KOD, 2004].....	25
• Figure 3.3:4: CCD charge transfer sequence in three-phase reader [KEV, 2004].....	26
• Figure 4.2:1: Block diagram of the CCD system [FAD, 2003].....	30
• Figure 4.3:1: The main components of CCD system.....	31
• Figure 4.4:1: Main components of interval generator box.....	32
• Figure 4.7:1: LabVIEW software interface.....	33
• Figure 4.8:1: CRO output showing the grab signal, held low for approximately 1 second to allow read out of video data.....	34
• Figure 4.8:2: Video and clock signal measurement to verify the dark current signal in room temperature.....	34
• Figure 4.8:3: Video signal from selected pixels were reached its saturation level at 500ns.....	35
• Figure 4.8:4: Clock signal serially read-out at clock speed of 1MHz. The clock signal was distorted from its initial square shape according to the problems with electronic system.....	35
• Figure 4.9:1: ^{14}C microscales was attached and fixed to the glass slide.....	36
• Figure 4.9:2: ^{14}C microscales was folded with scintillator paper and tape was used for easy handling using a tweezer. ^{14}C microscales was mounted on top of CCD image sensor.....	37
• Figure 4.10:1: Schematic diagram showing the expected signal detection process for ^{14}C	38

- **Figure 4.11:1:** A flow chart describes the post-acquisition process using Matlab software.....39
- **Figure 5.2:1:** The characteristic curve of dark current effects during the warming-up stage of the CCD in room temperature (Blue curve) and under cooled conditions in liquid nitrogen (Pink curve). The spread of the 20 data sets were presented in the mean pixel intensity. The standard deviation shows the minimum and the maximum value that were obtained from the 20 readings of mean pixel intensity for various exposure times.....42
- **Figure 5.3:1:** A single frame acquired shows different pattern for each particular source:
 - (i) Single image of ^{241}Am without scintillator paper. It was observed only a few bright spots stacked together throughout the CCD pixels.
 - (ii) Single image of ^{14}C microscales without scintillator paper. It was observed a formation of the bar with different brightness due to radiation exposures to the CCD pixels.....44
- **Figure 5.3:2:** A single frame acquired shows different pattern for each particular source:
 - (i) Single image of ^{241}Am folded with scintillator paper. The single frame displays many bright spots dispersed throughout the CCD pixels.
 - (ii) Single image of ^{14}C microscales folded with scintillator paper. The single frame clearly shows a formation of the bar with different brightness close to each other due to radiation exposures to the CCD pixels.....44
- **Figure 5.3:3:** A final frame acquired depends on the number of frames accepted during post-acquisition process:
 - (i) Final image of ^{241}Am without scintillator paper. The final image was zoomed in to observe if there is any central bright spots can be detected. No events (white spots) can be seen from the image.
 - (ii) Final image of ^{241}Am folded with scintillator paper shows central bright spots were detected. The white spots represent an event and the blue background as a noise.....45

- **Figure 5.3:4:** A final frame acquired depends on the number of frames accepted during post-acquisition process:
 - (i) Final image of ^{14}C microscales without scintillator paper. The white area was zoomed in from the final image to observe if there is any formation of the bars with the different brightness can be detected. No events (bars) can be seen from the image.
 - (ii) Final image of ^{14}C microscales folded with scintillator paper shows a formation of bar with different brightness were detected. The bars represent an event and the blue background as a noise.....46
- **Figure 5.3:5:** Histogram represents the true events counted in ^{241}Am when radiation deposited its energy in CCD sensitive volume. The minimum event counted as 0 is equal to the maximum event, 255 which means no events were detected for the final image in figure 5.3:3(i).....47
- **Figure 5.3:6:** Histogram represents the true events counted in ^{241}Am folded in scintillator paper when radiation deposited its energy in CCD sensitive volume. There were many events detected which varied from 0 to 255. As a result, in the final image as in figure 5.3:3(ii), we can observe many white spots.....47
- **Figure 5.3:7:** Histogram represents the true events counted in ^{14}C when radiation deposited its energy in CCD sensitive volume. As in figure 5.3:5, we are not able to see any event because of minimum and maximum event is almost same.....48
- **Figure 5.3:8:** Histogram represents the true events counted in ^{14}C folded in scintillator paper when radiation deposited its energy in CCD sensitive volume. We are able to see a few events which follow the pattern of beta energy (bars with different brightness) distribution throughout the CCD pixels.....48

List of tables

- **Table 1.2.2:1:** The Beta radioisotopes used with its various characteristic: half-life, mode of decay and energy. The top five are commonly used in beta autoradiography whereas some radionuclides emitting Auger electrons and gamma as well [JTO, 1999].....3
- **Table 2.1:1:** Comparison between the properties of autoradiography techniques [FAD, 2003].....10
- **Table 2.8:1:** Properties of digital autoradiography detectors.....19

Chapter 1

Introduction

1.1 Overview

Autoradiography was originated by the discovery of uranium nitrate and tartrate blackens silver chloride and silver iodide emulsions. The incident was noticed by Niepce de St. Victor in 1867 and similarly by Henri Becquerel in 1869, when he observed that opaque paper placed between the uranium nitrate and the emulsion experienced the same darkening effect [GAM, 2004].

The autoradiography technique initiated from this incident when Becquerel discovered the plates were darkened in the regions where radioactive materials were located. This agrees with the basic principle of autoradiography: the location of radioactivity specifically in biological materials is observed through dark spots on an emulsion film.

Autoradiography consists of the following parts: the biological samples, the radionuclide that is used as a tracer to label the sample, and the detecting medium which is a film in traditional method. Gradually, this conventional technique of autoradiography is being replaced by digital detectors. One of the most popular detector in digital autoradiography which will be described in this dissertation is Charge-Coupled Device (CCD) sensor.

1.2 Components of Autoradiography

1.2.1 Specimen / Sample

There are many types of specimen that are used in autoradiography either from biological organisms, chromatography or electrophoresis. The prepared samples should be very thin (~few μm) whenever the main interest is high resolution. The samples can be acquired from the entire organism (plant seeds up to animal) or just take slices of tissue.

Typically, a microscope is not necessary for the work of preparing specimens. The preparation of the samples in light microscopy (LM) autoradiography is about $\sim 0.5\text{-}5\mu\text{m}$ in thick. Electron microscopes are only used in ultra-thin sections, which is typically about 40-80 nm of plastic embedded material [JTO, 1999].

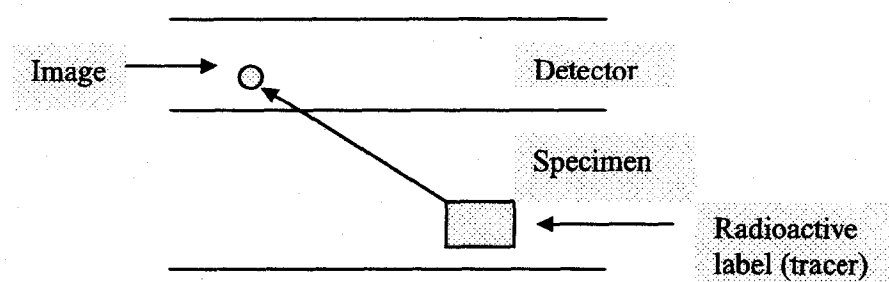


Figure 1.2.1:1: Autoradiography process involves specimen, tracer and detector to form the image [BAK, 1989].

1.2.2 Radionuclides

The main considerations that need to be taken into account when choosing the radioisotopes to perform autoradiography are the characteristics of the radiation emitted from the biological aspect. The most common radioisotopes used are ^3H and ^{14}C because both of them can easily be incorporated into nearly any organic molecules. However, the radioisotopes sometimes deemed unsuitable due to their low energy ($E_{\text{max}} \sim 18\text{-}156\text{ keV}$), where self-absorption in the sample of specimen can reduce the ability to detect radiation emission [GAH, 1972].

ISOTOPE	Half-life ($T_{1/2}$)	Decay	Energy
Tritium	12.35 years	β	18.6 keV (Max); 5.7 keV (Average)
Carbon-14	5760 years	β	156 keV (Max); 50 keV (Average)
Sulphur-35	87.4 days	β	167 keV (Max); 49 keV (Average)
Phosphorus-32	14.3 days	β	1.71 MeV (Max); 0.70 MeV (Average)
Phosphorus-33	25.5 days	β	248 keV (Max); 77 keV (Average)
Calcium-45	165 years	β	250 keV (Max)
Chlorine-36	3.03×10^5 years	β	714 keV (Max)
Strontium-90	28 years	β	540 keV (Max)
Iron-55	2.7 years	Auger e^-	5.5 keV
Iodine-125	60 days	Auger e^-	2.9 keV; 0.8 keV (X-ray present)
Cobalt-57	270 days	Auger e^-	14 keV (γ -ray present)
$^{99}\text{Tc}^m$	6.02 hours	γ	140 keV

Table 1.2.2:1: The Beta radioisotopes used with its various characteristic: half-life, mode of decay and energy. The top five are commonly used in beta autoradiography whereas some radionuclides emitting Auger electrons and gamma as well [JTO, 1999].

Instead of the half-life of the radioisotope, important parameters are the energy and type of particles emitted. Half-life is a measurement of the probability that a certain radioisotope will spontaneously decay to become half of its initial activity and emit particles. For the autoradiography purposes, the radioisotope's half-life should be long enough so that sufficient radioactivity still remains after sample processing but not too long for enough exposure.

1.2.3 Film

The film for autoradiography consists of three main layers: emulsion, base and protective coating. The emulsion layer usually 10-20 μm in thick and composed of silver halide grains (AgI, AgBr, AgCl) dispersed within gelatine. The larger grains show better

sensitivity but display low resolution. Conversely, smaller grains will produce the reverse effect.

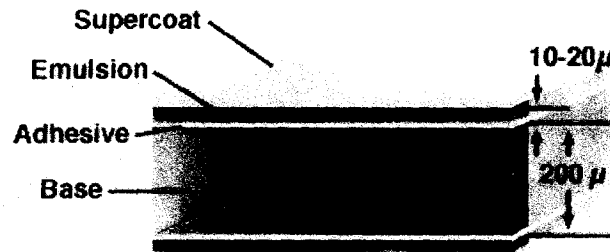


Figure 1.2.3:1: Cross-section of double coated photographic emulsion illustrating the base, emulsion and supercoat. The emulsion is attached to the base by a thin layer of adhesive [GAM, 2004].

The latent image formation is due to the oxidization of the bromine atoms, causing the release of free electrons. The free electrons travel through the crystal until it becomes trapped in one of the imperfection in the lattice. The electrons attract the silver ions, which reduce to silver atom and form clumps called latent image centers [ROG, 1967].

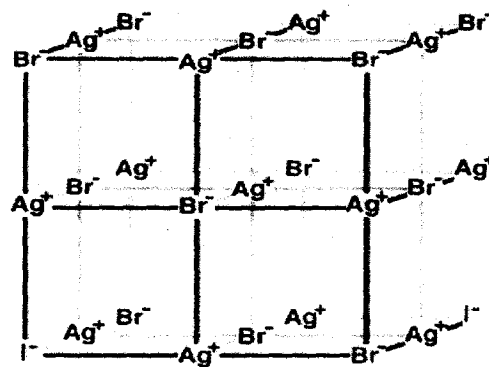


Figure 1.2.3:2: Silver halide crystal lattice structure showing the relative locations of Br⁻, Ag⁺ and I⁻ ions [GAM, 2004].

1.3 Techniques of Conventional Autoradiography

Most of the autoradiography experiments can be carried out in different ways according to the type of study performed and information required. Briefly, autoradiography is divided into

two subdivision, DNA sequencing and thin tissue imaging. In the early years, thin tissue autoradiography was performed either as macroautoradiography or microautoradiography. Over a few decades, light and electron microscopy autoradiography was introduced.

Autoradiography is a useful biological tool where organisms are screened to monitor the distribution of a wide variety of compounds including drugs, hormones and growth substances. It requires the entire organisms, or slices of whole organisms such as bone or leaves placed in close contact with film to produce an autoradiograph. The resolution level required by the macroautoradiography is less than microautoradiography. Macroautoradiography provides a spatial resolution of approximately 30 μ m [GAH, 1972].

In all types of autoradiography, there are different techniques of getting an exposure. The oldest and simplest method is through the direct contact method in which the specimen is just pressed directly onto the radiographic film or plate. After exposure, the film is separated from the sample and being developed. A factor that affects the quality of the images obtained is the uniformity of pressure between the sample and photographic material as well as the uniform thickness of the sample [VMR, 1966].

The other technique is by coating the sample with a liquid emulsion. This has added an advantage of autoradiography to be conducted on curved surface samples. By this technique, a melted photographic emulsion is poured onto the specimen, which means the emulsion will shape itself to the sample. Typically a layer of preparative coating is poured onto the specimen before the liquid emulsion, in order to give better adherence of the emulsion layer [BAK, 1989].

Other techniques used are base-free emulsion layer or more often recognized as the 'stripping film' technique and direct mounting method. In electron and light microscopy autoradiography, the samples thickness should be very thin to get higher resolution. The darkened grains have to be observed under an electron microscope or light microscope. Usually electron microscope is used in detecting the tracks of particles since these tracks are generally very short and small.

Resolution is defined as the capability to distinguish two nearest objects as separate. Basically, an increase in resolution means a decrease in sensitivity. The factors which may influence the resolution are isotope selection, distance from the source to the emulsion, the thickness of emulsion layer, exposure time, size of silver halide crystals and the ability of emulsion to detect emitted wavelength [GAM, 2004].

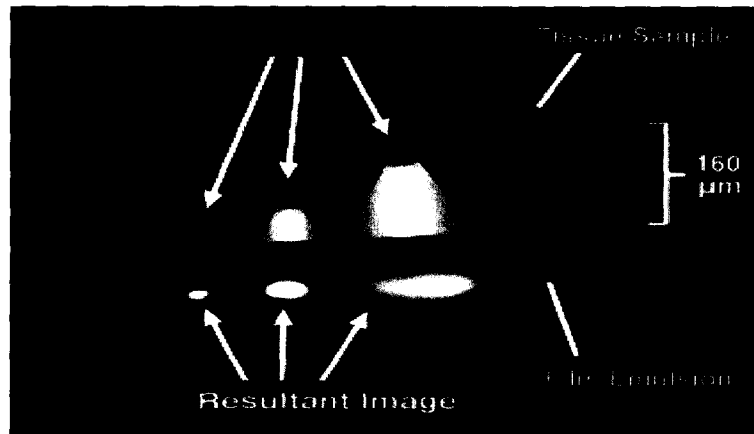


Figure 1.3:1: The effect of slice thickness on resolution. Emission sources that are distant from the photographic film (as in thick slices) may expose a broader area of the emulsion than sources that are close [GAM, 2004].



Figure 1.3:2: The effect of energy and tissue thickness on resolution. The top row of sections uses the low-energy emitter ^{14}C as a tracer; the bottom row uses the higher-energy emitter ^{18}F . Thicknesses of the sections in both rows are 20, 40, 120, and 180 μm from left to right. Resolution is degraded for the higher-energy emitter and diminishes as tissue thickness increases [GAM, 2004].

Achievable resolution is a function of electron energy (see figure 1.3:1) and slice thickness (see figure 1.3:2). High energy emissions will travel farther from their point of origin, and emissions from deep within a thick tissue section will subtend a greater angle as they reach the film. Since higher-energy emissions are attenuated less through thick slices than low energy emissions, resolution drop-off due to increasing slice thickness is more pronounced for high-energy emitters.

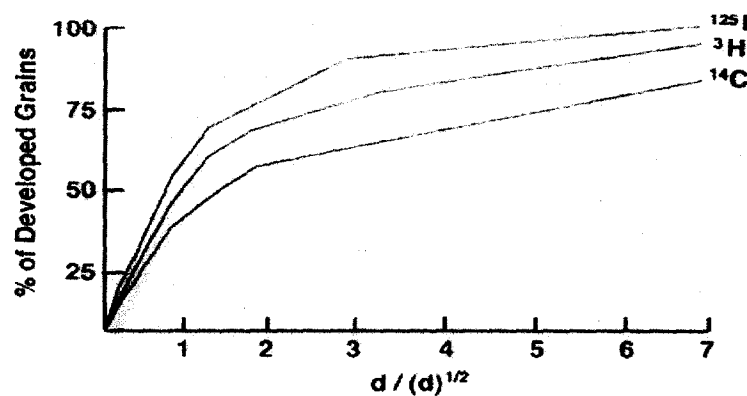


Figure 1.3:3: Distribution of tracks versus energy for microautoradiography. $d / (d)^{1/2}$ is the distance between a developed grain and its radioactive source divided by the median distance of all developed grains. The graph implies that it is more difficult to determine the origin of high-energy electron emitters than low-energy electron emitters due to longer tracks and wider track scattering [GAM, 2004].

Sensitivity can be improved by increasing the thickness of section. In addition, the larger the silver grains, meaning that more light will be absorbed. However, this is not applicable in microautoradiography, where number of grains per unit area is concerned. Therefore, sensitivity is assisted by smaller and more densely packed grains [GAM, 2004].

1.4 Advantages and disadvantages of Conventional Autoradiography

Conventional autoradiography is less expensive technique available which supplies an excellent spatial resolution of the images down to approximately 0.1 μm . As a result, it can be applied to produce the image even at sub-cellular levels.

Chapter 1 - Introduction

Besides a better spatial resolution, this technique suffers from poor sensitivity due to the low X-ray / beta particles detection efficiency. Integration period up to several months is required to exhibit satisfactory outcomes. Moreover, this technique also has a limited dynamic range (maximum 10^2) that may lead to under exposure or over exposure some sections of the image, comprising quantification of the absolute range of tracer concentration within the image [RJO, 2000].

The other drawbacks of conventional autoradiography are high background noise level $\sim 10^5$ events/mm², non-linear response of the film and does not provide any information for real time imaging. The need of chemical development of film could also be considered as a problem since many factors (e.g. temperature of developing solution) may transform the quality of the image.

References:

[BAK, 1989] John R.J. Baker

'Autoradiography: A Comprehensive Overview', Royal Microscopical Society, Microscopy Handbook 18, Oxford University Press, 1st Edition (1989).

**[GAH, 1972] T.C. Appleton, Rita Bogoroch, G.C.Budd, P.B.Gahan, S.R. Pelc,
Edited by P.B. Gahan,**

'Autoradiography for Biologists', Academic Press Inc. (London), 1st Edition (1972).

[GAM, 2004] Dr. Gambhir

'The Principles of Autoradiography', 2004 (22nd June 2004),

http://laxmi.nuc.ucla.edu:8248/M248_98/autorad/

[JTO, 1999] J.T. Ong

'Charge-coupled Device (CCD) in Autoradiography', University Of Surrey MSc Dissertation (1999).

[RJO, 2000] R.J. Ott, J. Macdonald, K.Wells

'The performance of a CCD digital autoradiography system', *Phys. Med. Biol.*, Vol. 45 (2000), pg. 2011-2027.

[ROG, 1967] Andrew W. Rogers

'Techniques of Autoradiography', Elsevier Publishing Company, Netherlands, 1st Edition (1967).

[VMR, 1966] Jaroslav Benes

Translated by V.W. Rampton,

'Fundamentals of Autoradiography', Iliffe Books Ltd, London (1966)